Quarterly Journal of the Royal Meteorological Society Tropical cyclone predictions over the Bay of Bengal using ...

yesu babu

RMetS
Royal Meteorological Society

Tropical cyclone predictions over the Bay of Bengal using the high-resolution Advanced Research Weather Research and Forecasting (ARW) model

C. V. Srinivas,[a]* D. V. Bhaskar Rao,[b] V. Yesubabu,[c] R. Baskaran[a] and B. Venkatraman[a]

[a]*Radiological Safety Division, RSEG Group, Indira Gandhi Centre for Atomic Research, Kalpakkam, India*
[b]*TLGVRC, Jackson State University, Jackson, MS, USA*
[c]*Computational Atmospheric Sciences Group, Centre for Development of Advanced Computing (C-DAC), Pune*

*Correspondence to: C. V. Srinivas, Radiological Safety Division, RSEG Group, Indira Gandhi Centre for Atomic Research, Kalpakkam 603102, India. E-mail: cvsri@igcar.gov.in

The performance of the high-resolution Advanced Research Weather Research and Forecasting (ARW) model for tropical cyclone prediction over the Bay of Bengal region of the northern Indian Ocean is assessed through study of 21 cyclone systems. Error metrics in the predicted fields of maximum sustained winds (MSW), central sea-level pressure (CSLP) and the vector track position are computed by comparison with corresponding tropical cyclone estimations from the India Meteorological Department (IMD). From 65 sensitivity experiments for five severe cyclones the combination of Kain–Fritsch (KF) convection, Yonsei University (YSU) planetary boundary layer (PBL), LIN explicit microphysics and NOAH land surface schemes are found to provide the best simulations for intensity and track prediction. It has been found that the KF convection scheme gives higher convective warming with stronger vertical motions relative to other tested cumulus schemes and that the YSU scheme simulates more realistic winds in the inflow region than other tested PBL schemes. Results of simulations with the best physics for all 21 cyclones reveal that the model had a tendency to overestimate the intensity, with mean errors ranging from −2 to 15 hPa for CSLP, 1 to 22 m s^{-1} for MSW corresponding to 24 to 72 h predictions. The mean vector landfall position errors are found to be 122 km at 12 h, 170 km at 24 h, 244 km at 48 h and 250 km at 72 h, and 67% of the landfall errors are less than 135 km, indicating fairly good forecasts. Further, the predictions are found to be best for northward moving cyclones followed by northwestward, westward and northeastward moving cyclones. Copyright © 2012 Royal Meteorological Society

Key Words: Tropical cyclones; Bay of Bengal; ARW model; numerical prediction

Received 23 April 2012; Revised 27 September 2012; Accepted 2 October 2012; Published online in Wiley Online Library

Citation: Srinivas CV, Bhaskar Rao DV, Yesubabu V, Baskaran R, Venkatraman B. 2012. Tropical cyclone predictions over the Bay of Bengal using the high-resolution advanced research weather research and forecasting model. *Q. J. R. Meteorol. Soc.* DOI:10.1002/qj.2064

1. Introduction

Tropical cyclones (TC) are highly disastrous weather phenomena causing damage to the life and physical infrastructure in tropical maritime countries. Accurate prediction of formation, movement and intensity of TCs is vital for early warning and disaster management, and is a challenging problem. Tropical cyclones form over warm tropical oceans and move towards the land under the action of steering forces (Gray, 1968). Extreme winds, heavy rainfall and associated storm surges generated on land fall characterize the cyclone damage potential. The Bay of Bengal (hereafter 'BOB') region of the northern Indian Ocean (NIO) is known to have high potential for cyclogenesis, with an annual frequency of about five cyclones (Bhaskar Rao *et al.*, 2001) that are highly variable in respect of movement and intensification (Raghavan and Sen Sarma, 2000), which necessitates application of suitable dynamical models for their prediction.

There has been remarkable advance in operational weather prediction models such as the US National Centers for Environmental Prediction's (NCEP) Global Forecast System (GFS), the European Centre for Medium-range Weather Forecasts (ECMWF) model, and the UK Meteorological Office model (UKMET). Parallel advancements in the development of sophisticated three-dimensional mesoscale models such as the US National Oceanic and Atmospheric Adminstration (NOAA) Geophysical Fluid Dynamical Laboratory's (GFDL) regional hurricane model, Weather research and forecasting (WRF) non-hydrostatic mesoscale models by the NCEP/NCAR (National Center for Atmospheric Research) have led to consistent improvement in the official TC forecasts by the national weather agencies both in USA and other tropical countries (Rappaport *et al.*, 2009).

Accurate numerical prediction of TCs is highly dependent on the quality of the initial state, resolving the *in situ* tropical cyclone circulation and the accurate representation of physical processes in the models. Although large-scale flow determines the motion of the cyclones, the inner-core dynamics and its interaction with the environment determine the intensity of the system (Marks and Shay, 1998; Davis *et al.* 2008). Forecasting the track and intensity of TCs is extremely important for the coastal region of India, more so for the east coast, due to the huge amount of damage inflicted by these storms on coastal habitat and agricultural resources, critical infrastructure facilities and other developmental activities. An important requirement is to obtain consistent forecasts on real time.

Several simulation studies have been conducted to study the TCs over the NIO using mesoscale models with the intention of evaluating them with respect to physics sensitivity, resolution, initial conditions and impact due to data assimilation, etc. (e.g. Mohanty *et al.*, 2004; Bhaskar Rao *et al.*, 2006, 2007, 2009; Prasad and Rama Rao, 2003; Trivedi *et al.*, 2006; Srinivas *et al.*, 2007, 2010; Deshpande *et al.*, 2010; Krishna *et al.*, 2010; Mukhopadhyay *et al.*, 2011; Singh *et al.*, 2008, 2011, 2012; Pattanik and Mohanty, 2008, 2010; Raju *et al.*, 2011a). Very few studies have reported the performance of numerical models statistically for the cyclones over the NIO. The India Meteorological Department currently uses a quasi-Lagrangian model for real-time operational forecasting of tropical cyclones over the NIO and the mean track errors are reported as 92, 152, 235 and 375 km corresponding to 12, 24, 48 and 72 h forecasts (Rama Rao and Prasad, 2005; Prasad, 2006; Prasad and Rama Rao, 2006; Tyagi *et al.*, 2010). Raju *et al.* (2011b) studied the performance of Advanced Research Weather Research and Forecasting (ARW) model using the 50 km resolution GFS model initial conditions for four cyclones in 2007–2010 and by comparing the winds and vector track positions with the Joint Typhoon Warning Center (JTWC) estimated values, which indicated mean track errors at landfall time as 98 km. All the above studies of TCs over the NIO are independent and different with respect to cyclone systems, sensitivity evaluations and with the model formulations (resolutions, physics, etc.), thereby making it difficult to arrive at definite conclusions. Moreover, no single study so far for the NIO region has been aimed at operational cyclone prediction issues, which require model evaluations considering the number of cyclones and quantitative assessments for obtaining mean error/uncertainty for operational forecasting purposes.

The National Hurricane Center (NHC) of NOAA and the National Weather Service (NWS) in the USA has been using the GFDL hydrostatic hurricane modelling system for the operational prediction of Atlantic TCs since 1995. With improvements in resolution and physics, the model has been shown to have produced improved skill in intensity and track forecasting since 2005. The GFDL model incorporates ocean–atmospheric coupling using the Princeton Ocean Model, improved physics, vortex initialization and fine horizontal resolution. Bender *et al.* (2007) provided a summary of the GFDL model advancements and its performance for the Atlantic and east Pacific TCs. The average track errors of the GFDL model are reported to vary from 72 km at 12 h to 340 km at 72 h for the Atlantic cyclones from 1996 and 2005. With the 2006 version of GFDL the average intensity errors are reported to have been reduced by 13% to 22%, with actual reduction in maximum winds by 1.3 m s^{-1} to 2.8 m s^{-1} at 24 h to 72 h forecasts for the Atlantic cyclones from 2004 to 2005. The improved performance of the GFDL model was attributed to the implementation of cloud microphysics and an improved surface momentum flux parametrization. The hurricane weather research and forecasting (HWRF) modelling system is a next generation non-hydrostatic hurricane model developed by NOAA and implemented as an operational hurricane model by NCEP. McNoldy *et al.* (2010) have studied the performance of HWRF for the 2009 Hurricane season and showed that the HWRF and GFDL models performed similarly for the first 24 h, HWRF out-performed GFDL during 24–72 h, and GFDL out-performed HWRF during 72–120 h. In terms of track errors, HWRF and GFDL performed similarly up to 72 h, then GFDL was better than HWRF during 72–120 h. The average track errors for the 2009 hurricanes as simulated by the HWRF model were reported to range from 92 km at 24 h to 518 km at 120 h forecasts and corresponding intensity errors varied from 7 m s^{-1} at 24 h to 12 m s^{-1} at 120 h forecasts. The high bias in forecast intensity was attributed to the weak cyclonic systems in hostile environments. Yeh *et al.* (2011) studied the real-time forecasts from an experimental version of HWRF called HWRFX with two domains (27 and 9 km horizontal resolution), using slightly different physics for Atlantic hurricanes in 2008 and considering a sample of 57 to 20 cases for 12 h to 120 h forecasts. It was found that the performance of HWRFX is comparable to the NOAA operational models in terms of the accuracy for both track and intensity forecasts, but with a negative bias in the intensity forecasts as opposed to the positive bias of the NOAA operational models. The average track errors for the 2008 hurricane season with HWRF/HWRFX were found to range from 37.5/42.6 at 12 h to 286.2/260.9 km at 120 h forecasts and the corresponding mean intensity errors varied from 3.69/4.5 m s^{-1} at 12 h to 11.6/12.7 m s^{-1} at 120 h. The negative bias with HWRFX using the GFDL initial conditions was attributed to inconsistencies in dynamics between the two models. Zhang *et al.* (2011) studied the impact of high resolution (3 km) on the experimental hurricane modelling system (HWRFX) considering 10 different tropical cyclones during the 2005 and 2007. The absolute track errors were shown to be about 50/55 km at 12 h increasing linearly to 560/530 km at 120 h forecast and the intensity was reported to vary as 12/8 m s^{-1} at 24 h to 14/13 m s^{-1} at 120 h with 9 km/3 km resolution forecasts respectively. Gopalakrishnan *et al.* (2012) evaluated the performance of the experimental high-resolution HWRFX model for 87 cases of Atlantic tropical cyclones during the 2005, 2007 and 2009 hurricane seasons with two versions of horizontal resolutions (27–9 km and 9–3 km) using different initial conditions from the operational GFDL and HWRF models and with sensitivity tests for the model physics. It was shown that the 9–3 km HWRFX system using the GFDL initial conditions and the model physics similar to the operational version of HWRF provides the best results in terms of both track and intensity prediction. In their study it was found that the average track errors for the various operational models (GFDL, HWRFX) increase almost linearly from near 60 km at 12 h to 529 km at 120 h using the 9 km grid resolution in HWRFX. It was shown that although GFDL provided the best performance through the forecast length, the high-resolution HWRF (3 km resolution) provided the next lowest track errors of 90 km at 24 h increasing to 320 km at 120 h. As for intensity, the 9 km HWRF with HWRF initial conditions produced the best predictions, with average intensity errors ranging from 9 m s^{-1} at 24 h to 13 m s^{-1} at 120 h. Davis *et al.* (2008) tested the ARW model for real-time simulations of five landfalling hurricanes in the Atlantic basin and showed that the predictions were generally competitive and occasionally superior to the operational forecasts with GFDL, NOGAPS, UKMO, AVNO and other models. The average track error with ARW using 12 km/4 km resolutions for 2005 hurricanes were shown to be 35/25 km at 12 h gradually increasing to 135/120 km at 120 h, and the average intensity errors were reported to be 17/14 m s^{-1} at 12 h to 10/16 m s^{-1} at 96 h respectively.

The preceding review shows that research studies on TC prediction over the NIO as being mostly limited to single case studies, thus not providing an assessment of the prediction skill, in contrast to the significant research work using variations of the WRF modelling systems (ARW/HWRF/HWRFX) considering multiple tropical cyclone case studies. The main objective of this work is to quantitatively assess the skill of the ARW mesoscale model for TC track and intensity predictions over the BOB region considering a set of 21 cyclones that formed during the period from 2000 to 2011. Towards this objective, the best model physics is first identified by conducting sensitivity experiments considering a set of five severe cyclones (Nargis, Sidr, Khaimuk, Jal, Thane). The results are then evaluated statistically for all 21 cyclones considering the metrics of mean, root mean square error (RMSE) and standard deviation of the different storm parameters to assess the model skill. Section 2 provides a brief description of the storms considered in the evaluation; section 3 details the model configuration, initialization and description of numerical experiments; section 4 provides the results of sensitivity experiments; section 5 details the track and intensity errors for the 21 cyclones; and section 6 considers the simulation of the cloud and rain band structures of a few cases.

2. Description of the storms

A set of 21 tropical cyclones formed over the BOB during 2000 to 2011 are considered in order to assess the model skill for cyclone forecasts (Table 1 and Figure 1). Of these 21 storms, eight had cyclone intensity with wind speeds(34–47 knots) and the rest were severe to very severe cyclones that had maximum sustained wind speeds of (> 48 knots). The details of these storms are given in the annual bulletins of the Regional Specialized Meteorological Centre (RSMC) – Tropical Cyclones, New Delhi (India Meteorological Department, 2010). For the purpose of analysis we categorized the cyclones into three classes based on their movement and location of land fall, namely: (i) westward moving storms with land fall between 5° and 15°N; (ii) northwestward moving storms with land fall between 15° and 20°N; and (iii) northward/northeastward moving (land fall between 20° and 25°N). The cyclones considered for simulation are listed in Table 1 with details of time of occurrence, life span, direction of movement, landfall position and intensity category. Among these, five severe cyclones with land fall in four different regions (Jal, South Andhra coast; Thane, Tamilnadu coast; Khaimuk, Andhra coast; Sidr, Bangladesh coast; Nargis, Myanmar coast) are chosen for sensitivity experiments. Cyclone Sidr formed as a low pressure over southeast BOB and its life cycle was 11–16 November 2007. It progressively intensified into a very severe cyclonic storm at 1800 UTC on 12 November and crossed west Bangladesh coast with northward movement around 1700 UTC on 15 November. Cyclone Nargis formed as a depression over the southeast BOB on 27 April 2008 and intensified into a very severe cyclonic storm at 0300 UTC on 29 April. It moved in a northwestward and then northeastward direction and crossed the southwest coast of Myanmar near 16°N between 1200 and 1400 UTC on 2 May 2008. Cyclone Khaimuk originated as a low pressure on 12 November 2008 in the southeast BOB, intensified into a strong cyclone on 14 November over the west-central BOB and crossed the coast of south Andhra Pradesh on 15 November 2008. Cyclone Jal in the BOB had its life cycle during 4–7 November 2010, with a minimum central sea-level pressure (CSLP) of 950 hPa and maximum sustained wind speed (MSW) of 68 m s^{-1} (∼136 knots). Cyclone Thane formed as a depression on 25 December 2011 in the southeast BOB, progressively intensified as a very severe cyclone, moved in a north-northwesterly direction and crossed North Tamilnadu and Puducherry coast on 30 December 2011.

3. Model configuration, initialization and numerical experimentation

3.1. Model

The ARW version 3.2 mesoscale model (Skamarock *et al.*, 2008) is used in this study. The ARW model incorporates fully compressible non-hydrostatic equations and uses a terrain-following vertical coordinate. The model is versatile with a number of options for nesting, boundary conditions, data assimilation and parametrization schemes for subgrid-scale physical processes. In the present study ARW model

Table 1. Tropical cyclones formed in the Bay of Bengal (BOB) between 2000 and 2011 considered in the study.

Case	Period	Name	Landfall	Origin in BOB	Category*	Group†
1	27–30 December 2011	Thane	Pondicherry	South	SCS	A
2	17–20 May 2010	Laila	Machilipatnam AP	South	SCS	A
3	4–8 November 2010	Jal	Chennai	South	SCS	A
4	11–16 December 2009	Ward	Srilanka	South	C	A
5	23–26 May 2009	Aila	Sagar Island West Bengal	Central	SCS	A
6	24–27 November 2008	Nisha	Karaikal,TN	Southeast	SCS	A
7	13–16 November 2008	Khaimuk	Ongole, AP	Central	C	A
8	24–27 October 2008	Rashmi	Bangladesh	Central	C	C
9	28 April–2 May 2008	Nargis	Myanmar	Central	SCS	C
10	12–15 May 2007	Akash	Bangladesh	Central	SCS	C
11	13–16 November 2007	Sidr	Bangladesh	Southeast	SCS	C
12	26–29 April 2006	Mala	Myanmar	Central	SCS	C
13	7–10 December 2005	Fanoos	Dhanushkoti, Tamilnadu	South-central	C	A
14	28 November–1 December 2005	Baaz	No landfall	Central	C	A
15	17–21 September 2005	Pyarr	No landfall	Southeast	C	A
16	16–19 May 2004	Myanmar-04	Mynmar	North	SCS	C
17	13–16 December 2003	Machilipatnam	Machilipatnam, AP	Southeast	SCS	B
18	24–27 November 2002	Myanmar-02	Myanmar	Central	C	C
19	10–13 November 2002	Bangladesh 02	Bangladesh	Southwest	SCS	C
20	27–30 November 2000	Cuddalore	Cuddalore, TN	Southeast	SCS	B
21	25–28 November 2000	Bangladesh-00	Bangladesh	East	C	C

* C, cyclone; SCS, severe cyclonic storm.
† A, northwestward; B, westward; C, northward.

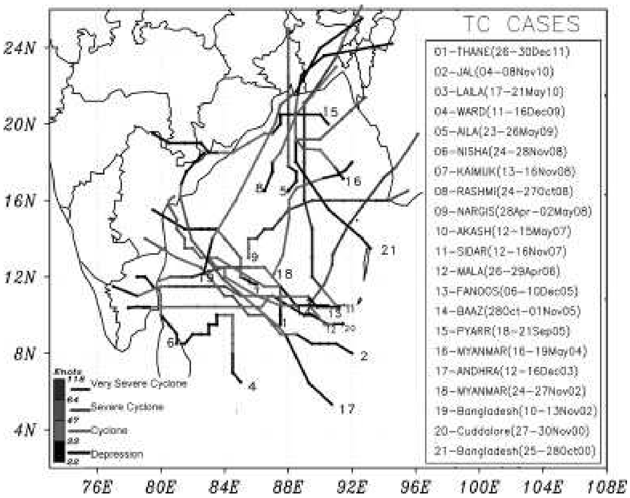

Figure 1. Actual tracks and intensities (from the IMD best track data) of the 21 tropical cyclones used in this study. The legend gives the best track maximum surface (10 m) wind speeds (in knots).

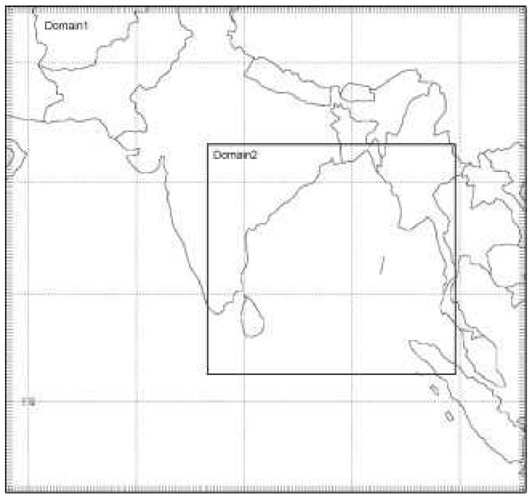

Figure 2. Domains used in the ARW model.

is configured with two-way interactive nested domains (Bhaskar Rao *et al.*, 2009). The outer domain covers a larger region (58.02°E to 105.97 E; −8.26 to 34.31°N) with 27 km resolution and 173 × 162 grids. The inner domain has 9 km resolution with 249 × 239 grids covering the BOB and its environment (77.9–99.40°E; 4.49–23.60°N; Figure 2). A total of 28 vertical levels are used with the model top at 100 hPa. The 27 km, 9 km horizontal resolutions are chosen as they are optimized for TC predictions by the NCEP for the operational HWRF model (McNoldy *et al.*, 2010; Yeh *et al.*, 2011; Zhang *et al.*, 2011; Gopalakrishnan *et al.*, 2012).

3.2. Model initialization

The terrain data (elevation, land use and soil types) in the model is defined from the US Geological Survey topography data at 10′ and 5′ resolutions for the outer and inner domains. The initial and boundary conditions are obtained from global operational analysis and forecasts of NCEP-GFS available at 1° × 1° latitude/longitude resolution and 6 h interval for the 15 cyclone cases in the period 2005–2011 (Table 1). As GFS data are not available for the period 2000–2004, the NCEP 6 h final analysis (FNL) data available at 1° × 1° degree resolution are used for initial/boundary conditions for the 6 cyclones during this period. The time-varying sea-surface temperature (SST) data over all the domains are also defined from the GFS/FNL data for respective cases. The model is integrated for 96 h for each cyclone. The data on the intensity and the position of the simulated cyclones are taken from the IMD reports for model evaluation. Rainfall observations at the coastal stations as available from IMD reports and Tropical Rainfall Measuring Mission (TRMM) satellite rainfall data sets are used for validation of simulated rainfall.

3.3. Numerical experiments

Numerical prediction of TCs needs suitable parametrizations for planetary boundary layer (PBL) turbulence, surface fluxes, cumulus convection (CC) and cloud microphysics (CMP) because these processes act together to influence the forecasts. Stronger cyclones provide a basis to evaluate the parametrizations because the structure and intensification processes are dependent on the physics. In the present study the ARW model is first evaluated for sensitivity to physics (convection, PBL diffusion, CMP, surface processes) considering a set of five severe cyclones (Nargis, Sidr, Khaimuk, Jal, Thane) from the 21 cyclones listed in Table.1 Although it is desirable to evaluate each combination of physical packages for the entire sample of storms to have more statistically significant results on the set of best physics, a sample of only five severe cyclones with movement in four different directions are considered here to study the sensitivity to physics parametrizations, due to lack of computational resources.

The modelling incorporated the following: for convection, the KF (Kain, 2004), BMJ (Betts and Miller, 1986; Janjić, 2000), GDE (Grell and Dévényi, 2002) and Grell-2 (NG: New Grell) schemes; for PBL the Yonsei University (YSU; Hong *et al.*, 2006), MYJ (Mellor and Yamada, 1982; Janjić, 2002) and Asymmetrical Convective Model version 2 (ACM; Pleim, 2007) schemes; for cloud microphysics the LIN (Lin *et al.*, 1983), WRF single moment 3-class (WSM3; Hong *et al.*, 2004) and WRF Single moment 6-class (WSM6; Dudhia *et al.*, 2008) schemes; and for surface processes the five-layer soil thermal diffusion model (SOIL; Dudhia, 1996), the NOAH land surface model (Chen and Dudhia, 2001) and rapid update cycle model (RUC; Smirnova *et al.*, 2000). As mentioned earlier, a total of 13 simulations were conducted for each of the five TCs, with a sequential order of (i) cumulus convection, (ii) microphysics, (iii) PBL turbulence and (iv) land-surface physics, such that the best CC scheme is identified first, followed by CMP sensitivity experiments with only the best CC in order to identify the best CMP scheme; the selected CC and CMP schemes are then used for three PBL sensitivity experiments, followed by surface processes sensitivity experiments with the selected CC, CMP and PBL schemes.

The convection schemes compute vertical fluxes due to updrafts and downdrafts and compensating motion outside the clouds. They provide vertical heating and moistening profiles. In the Grell scheme, clouds are represented as two steady-state circulations caused by updraft/downdrafts with use of the Arakawa–Schubert type quasi-equilibrium assumption for closure (Arakawa and Schubert, 1974), wherein the rate of destabilization due to large-scale forcing equals stabilization due to convection. The KF scheme follows a Lagrangian parcel method and uses a simple cloud model with moist updrafts and downdrafts, including the effects of detrainment and entrainment. It has a trigger function, a mass flux formulation and closure based on convective available potential energy (CAPE). Its activation at a particular grid point is decided by the vertical velocity. The BMJ scheme is a convective adjustment scheme where the convection is initiated by buoyancy and does not include a cloud model. The convection profiles and the relaxation time depend on a non-dimensional parameter called 'cloud efficiency' (a function of entropy change, precipitation, mean temperature of the cloud; Janjić, 1994). The shallow convection moisture profile is related to the small and non-negative entropy change (Janjić, 1994). It does not include downdrafts and its activation at a particular grid point is determined by the thermodynamics. The Grell–Devenyi scheme uses an ensemble method in which multiple cumulus schemes of mass-flux type (with differing updraft and downdraft entrainment and detrainment parameters, and precipitation efficiencies) are run within each grid box and then the results are averaged to give the feedback to the model.

Of the three CMP schemes, WSM3 uses prognostic equations for water vapour, cloud water/ice and rain/snow, and both the WSM6 and Lin schemes include mixed-phase processes and predict six hydrometeors: water vapour, cloud water, cloud ice, rain, snow and graupel.

The PBL schemes provide the flux profiles within the boundary layer and stable layer and give the tendencies of temperature, moisture and horizontal momentum vertically. The physical bases of the three PBL schemes are as follows. The YSU scheme is a first-order non-local diffusion scheme which includes a parabolic type k-profile plus counter gradient terms to account for the transport of heat and moisture arising from large-scale eddies. The turbulent exchange coefficient is determined from the friction velocity, PBL height for momentum and from a Prandtl number relationship for temperature and moisture. This scheme uses an explicit entrainment layer at the PBL top calculated as proportional to the surface buoyancy flux. The MYJ scheme uses a level 2.5 turbulence closure (Mellor and Yamada, 1982) based on turbulent kinetic energy (TKE), length scale and use of local vertical mixing within the PBL (Janjić, 2002). The ACM scheme computes eddy diffusion (local method) in the stable conditions and non-local transport in unstable conditions; the partitioning between the two components is derived from the fraction of non-local heat flux according to the model of Holtslag and Boville (1993).

The surface layer schemes selected are the MM5 similarity scheme in combination with YSU, Pleim-Xue surface layer scheme (Pleim, 2006) with ACM and the Eta surface layer scheme with MYJ PBL as per their compatibility for the calculation of the friction velocity and the surface exchange coefficients for heat, moisture and momentum.

The land-surface models (LSMs) compute the surface heat and moisture fluxes to the PBL using information from the surface layer, the soil and land-use characteristics. The sensitivity of land-surface schemes is tested with three schemes: the SOIL model (Dudhia, 1996), the NOAH model (Chen and Dudhia, 2001) and the RUC model (Smirnova *et al.*, 2000). The SOIL scheme solves the thermal diffusivity equation using five soil layers and computes the fluxes of radiation, and sensible and latent heat fluxes. It parametrizes the soil moisture and snow content from land-use type. The NOAH model solves time-varying soil moisture and soil temperature with four layers and accounts for vegetation canopy effects. The RUC model is similar to NOAH but uses six soil layers and includes the effects of vegetation, canopy water and snow. The rapid radiation transfer model (RRTM) for long wave radiation (Mlawer *et al.*, 1997) and Dudhia's (1989) scheme for shortwave radiation are used in the model in all the sensitivity tests. For each of the selected five cyclones a total of 13 sensitivity experiments are conducted, that is, four for cumulus convection (KF, BMJ, GDE, NG), three for microphysics (LIN, WSM3, WSM6), three for PBL (YSU, ACM, MYJ) and three for surface processes (SOIL, NOAH, RUC). The error estimates for CSLP, maximum winds and track position in each case of simulation are derived as the difference between the IMD best-track parameter data and corresponding model value. The errors are averaged for all five cyclones in the evaluation of sensitivity experiments. With the identified best physics parametrizations, simulations are made for each cyclone listed in the Table 1 to evaluate the model performance.

4. Results from sensitivity experiments

Model sensitivity is first studied with respect to various physics parametrization schemes by conducting numerical experiments considering changing convection, microphysics, PBL and surface schemes to identify the best scheme every time. These experiments are categorized into four groups in order to study the sensitivity of the simulated features of the storm to the parametrization of convection, microphysics, PBL and surface processes. For intensity, CSLP, MSW and vector track positions are used as parameters for comparison with the respective reported values from the IMD. The model errors for each parameter are estimated as the difference between the IMD value and the corresponding predicted value. The mean error metrics (i.e. IMD value minus model value) from these groups are presented first in order to determine the best parametrizations for intensity and track estimates. To examine the reasons for the relatively better performance of various physics the results from the very severe cyclone Sidr are analysed.

4.1. Sensitivity experiments with convection schemes

Here, the convection schemes considered are the KF, NG, GDE and BMJ. To start with, the WSM6 scheme for microphysics, YSU for PBL and NOAH for surface physics are chosen because this combination has achieved the best performance in previous studies (e.g. Krishna *et al.*, 2012; Mukhopadhyay, 2011; Raju *et al.*, 2011a). The 6 h time variation of mean errors (i.e. IMD value minus model value) for all five cyclones in CSLP, MSW and track positions, along with the ensemble mean, are presented in Figure 3. It can be noted that CSLP is underestimated (higher intensification) with KF and overestimated (lesser intensification) with BMJ, GDE and NG (Figure 3(c)). Correspondingly, simulated maximum winds are underestimated with the BMJ, GDE and NG schemes and overestimated with the KF scheme (Figure 3(b)). The absolute mean errors for CSLP and wind are relatively less with the KF scheme than the other three schemes. The time variation of wind and pressure errors indicates that KF produces higher intensification and results closer to observations relative to other convection schemes.

From the time evolution of CSLP and 10 m maximum surface winds for cyclone Sidr (Figure 4) the intensity of the simulated storm is noted to be underestimated with the BMJ, NG and GDE convection schemes. The reported maximum pressure drop associated with the storm was 61 hPa, and simulated results are 58 hPa with GDE, 46 hPa with KF, 34 hPa for NG and 16 hPa for BMJ, indicating relatively better results with the GDE and KF schemes. The CSLP with the BMJ and NG schemes showed larger errors from 24 h onwards. The mature stage of the storm was about 14 h for GDE and about 10 h for KF. The observed lowest CSLP of the storm was 945 hPa at 72 h of model integration time, which was very nearly simulated by the experiment with the GDE scheme, followed by the KF scheme. The time variation of MSW (Figure 4(b)) indicates higher winds with KF and GDE (60 m s^{-1}) and relatively lower winds with other schemes (NG, 45 m s^{-1}; BMJ, 38 m s^{-1}). The time evolution of maximum winds with the KF scheme was closer to the IMD observations throughout the simulation, while the GDE experiment underestimated the winds till 50 h of integration. In contrast to the GDE and KF experiments, simulations with the NG and BMJ schemes significantly underestimated the winds throughout the simulation. Thus of the four cumulus schemes tested, the KF scheme produces an intense storm closely agreeing with the IMD estimates of winds and CSLP, whereas the others produce relatively weaker storms.

This is supported by the radius–height cross-sections of azimuthally averaged tangential winds (Figure 5), and by temperature anomaly and vertical wind data (Figure 6) for cyclone Sidr at its mature stage (0000 UTC on 15 November 2007). The wind distribution around the storm indicates that the KF scheme simulated the strongest cyclonic winds (70–100 m s^{-1}) vertically up to about 10 km in the troposphere and horizontally in a radius of about 150 km, followed by the NG, GDE and BMJ schemes. The tangential winds throughout the troposphere are stronger with the KF and NG schemes and relatively weaker with the BMJ and GDE schemes. The core of strong tangential winds in the BMJ experiment is limited to just 3 km and hence indicates a very weak storm relative to the other convection schemes. The central calm wind region is very narrow, indicating stronger intensity in the KF and NG experiments, with winds of the order of 5 m s^{-1} confined to a limited region of radius 0.25°. Gradual upward expansion of the calm wind region is seen coinciding with the outflow region.

The temperature anomaly (i.e. temperature deviation from the surrounding environment) shows the occurrence of a maximum warming of about 3.5 K in the layer of ∼8–10 km, up to 4 K in the layer of 6–13 km, up to 4 K in the layer of 3–15 km and up to 4 K in the region 2 to 15 km with the BMJ, GDE, NG and KF schemes respectively, indicating stronger convection and so a higher warming in the upper tropospheric region with the two latter schemes. A stronger vertical motion (2.0–3.0 m s^{-1}) prevailed in the KF simulation relative to other experiments up to 14 km height in the 20–50 km radius due to strong vertical updrafts in the eyewall region. The downward motion in the core region is also stronger with the KF scheme relative to the others.

The better performance of the KF scheme is related to the inclusion of updrafts, downdrafts and shallow convection processes and may be due to triggering of convection based on buoyancy. Because of widespread upward motion induced by convergence and the initial presence of minimal convective inhibition, the KF scheme becomes widely active and thus promotes deep convection in simulations. The NG scheme, although including downdrafts, does not activate enough (could be due to quasi-equilibrium assumption) to suppress grid-scale overturning thus simulating weak storms. The GDE scheme being an ensemble scheme averages out the effects of different schemes (with differing updraft and downdraft entrainment and detrainment properties, and precipitation efficiencies) and thereby reduces the net convective tendency as more suitable for stratiform convection.

The mean vector track errors at different integration times from experiments with different convection schemes

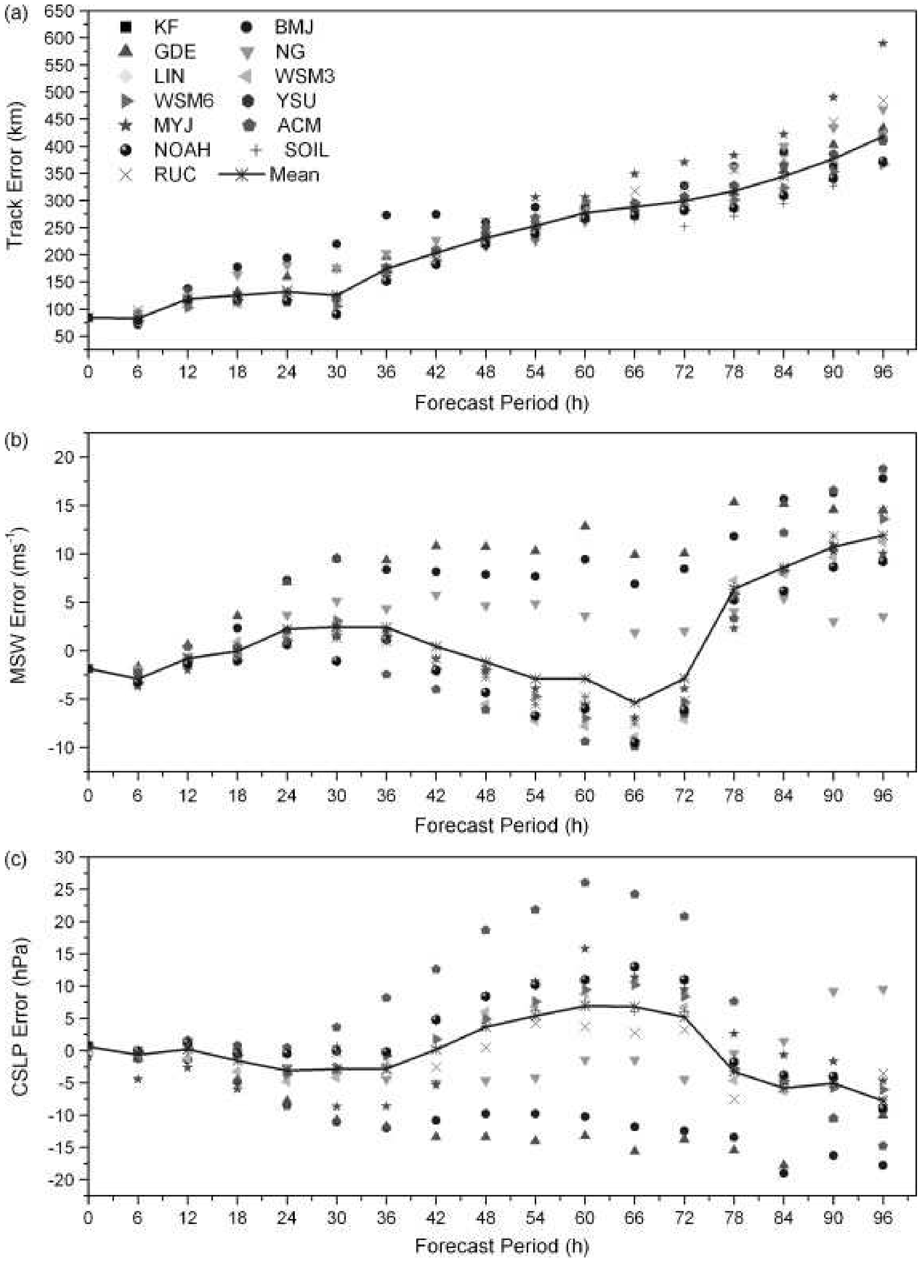

Figure 3. Time variation of mean errors for (a) vector track position (km), (b) maximum sustained winds (m s^{-1}) and (c) central sea level pressure (hPa) from the 13 physics sensitivity experiments for the five severe cyclones (Sidar, Nargis, Khaimuk, Jal, Thane).

indicate that the KF has smaller error than the GDE, BMJ and NG schemes. The track errors with the BMJ, GDE and NG schemes are higher by about 30–50% at 24 h, about 30% at 48 h, about 60–100% at 72 h and 96 h than with the KF scheme (Figure 3(a)). Time series of track errors for cyclone Sidr from experiments using different convection schemes (Figure 4(c)) indicate that the track errors progressively increased in the BMJ, GDE and NG experiments. These results indicate that the KF convection scheme provides the best simulation with minimum vector track errors and best estimation of the intensity.

4.2. *Sensitivity experiments with microphysics schemes*

Based on the results described in the previous section, further simulations were conducted with the KF convection, YSU PBL and NOAH surface schemes by varying the microphysics as according to the LIN, WSM3 and WSM6 schemes. All three microphysics schemes underestimated the CSLP (positive errors) and overestimated the winds (negative errors), thus simulating overintensification of the cyclones from 36 h onwards. Of the three schemes, the LIN scheme produced the least errors (< 15–20%) in CSLP compared with the WSM3 and WSM6 schemes, as well as in the simulated winds. Time series of model-derived CSLP and maximum winds for cyclone Sidr indicate (Figure 7) that the WSM3 simulation produced a relatively weaker cyclone throughout, except at 54 h where it had the value of 963 hPa for CSLP, and also weaker winds than with the LIN and WSM6 simulations. Both LIN and WSM6 schemes produced almost similar results for the CSLP, maximum winds and cyclone track errors. Of these two experiments LIN produced relatively higher intensification of the storm till 72 h of model integration, both in terms of central pressure and maximum winds closer to the IMD reported values. After 72 h the WSM6 produced higher intensification

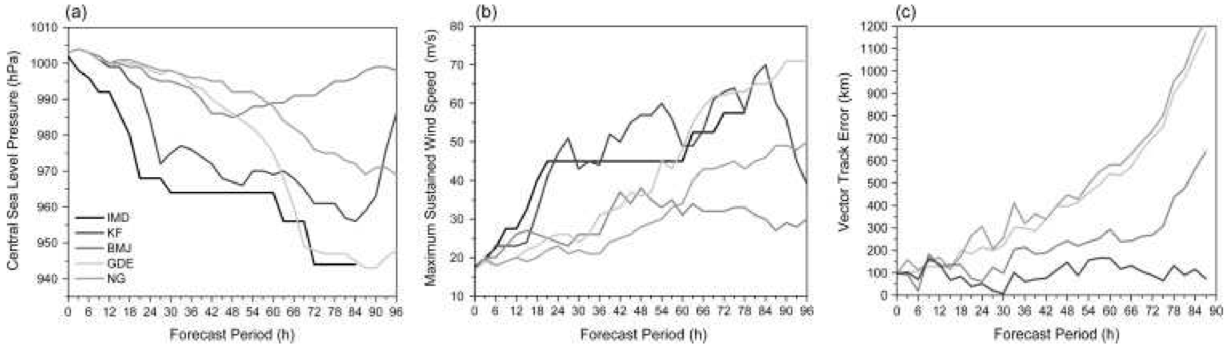

Figure 4. Time variation of simulated (a) central sea-level pressure (hPa), (b) maximum sustained winds (m s^{-1}) and (c)error in track positions of cyclone Sidr for the experiments with different convection schemes along with the IMD estimates.

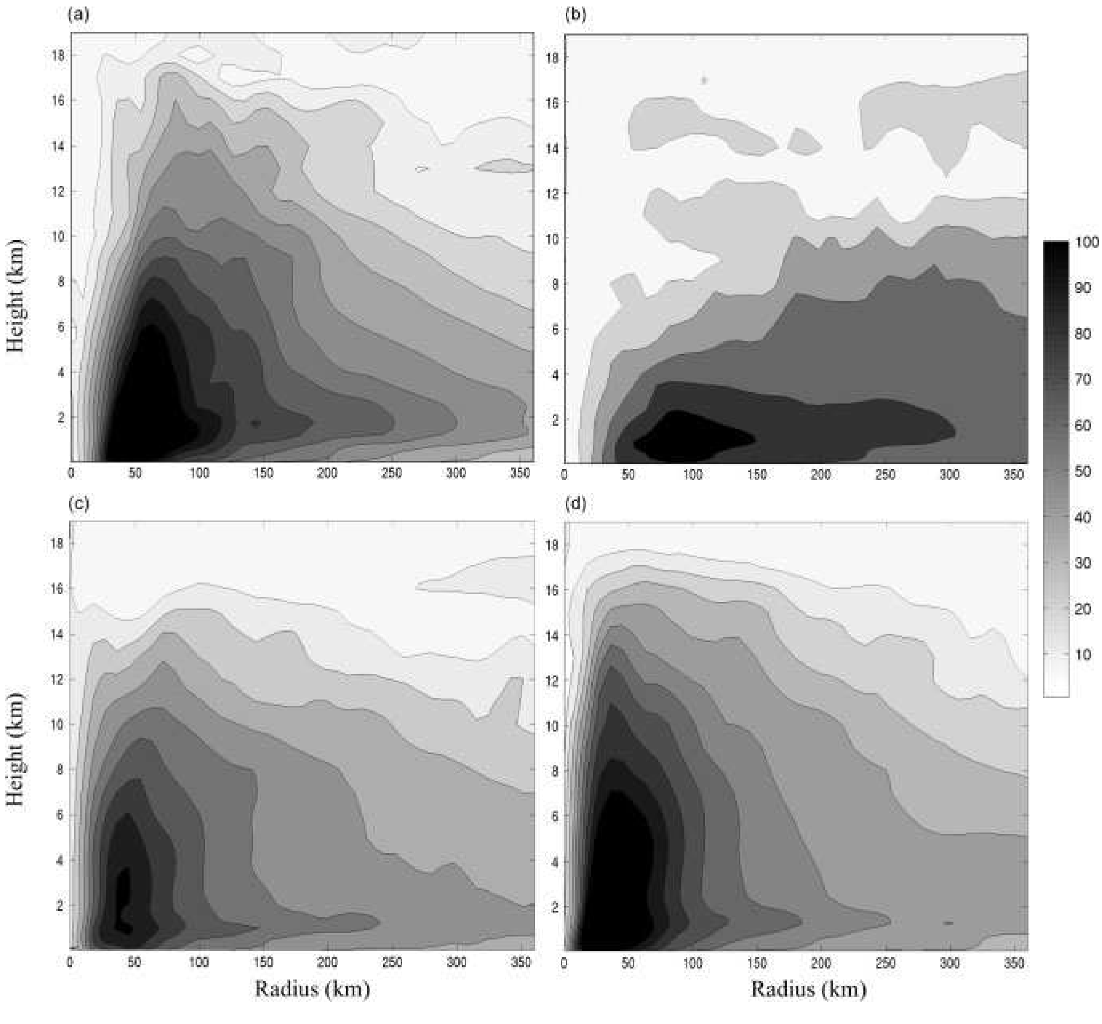

Figure 5. Depiction of the azimuthally averaged radius–height cross-section of tangential wind (m s^{-1}) from experiments with different convection schemes ((a) KF, (b) BMJ, (c) GDE and (d) NG) at the mature stage of cyclone Sidr corresponding to 0000 UTC on 15 November 2007. The scale on the *y* axis is height (km) and on the *x* axis is distance (km).

with a CSLP of 955 hPa and maximum winds of 72 m s^{-1}. Though the time series of CSLP is better simulated by WSM3 till 54 h, a rapid weakening (or rise in CSLP) was noticed thereafter in contrast to the observations. The time series of maximum winds with the WSM6 and LIN schemes till 48 h are nearly the same, and the LIN scheme produced relatively higher winds beyond 48 h till 72 h. The WSM3 gives unrealistic intensification before 48 h and weakening of the storm after 60 h.

The mean vector track errors between 24 and 96 h of integration time varied from 94 km to 450 km in experiments using different microphysics schemes. Although the errors with all three schemes are similar up to 24 h, the WSM3 and WSM6 schemes produced relatively higher track errors subsequent to 24 h, higher by about 10% at 24 h and 50% at 96 h than those obtained with the LIN scheme. The time series of the errors in track positions shown for cyclone Sidr indicates that the errors are least with LIN, whereas they gradually increased with the WSM3 and WSM6 schemes (Figure 7(c)). Thus with the combination KF convection scheme, LIN microphysics is preferred to the WSM3 and WSM6 schemes as it produced minimum track errors and

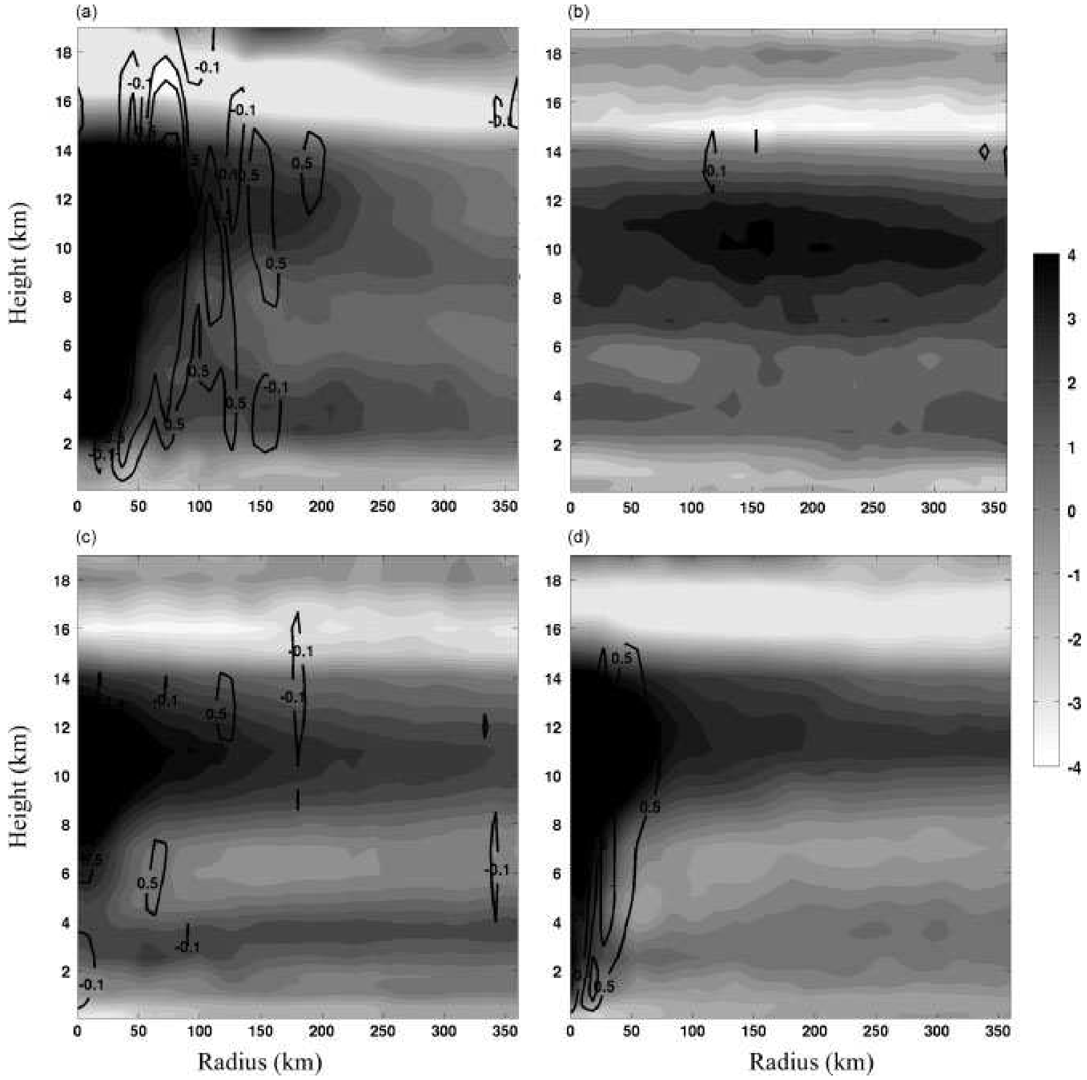

Figure 6. Depiction of the azimuthally averaged radius–height cross section of simulated temperature anomaly and vertical winds (m s^{-1}) from experiments with different convection schemes ((a) KF, (b) BMJ, (c) GDE and (d) NG) at the mature stage of cyclone Sidr corresponding to 0000 UTC on 15 November 2007. The scale on the *y* axis is height (km) and on the *x* axis is distance (km).

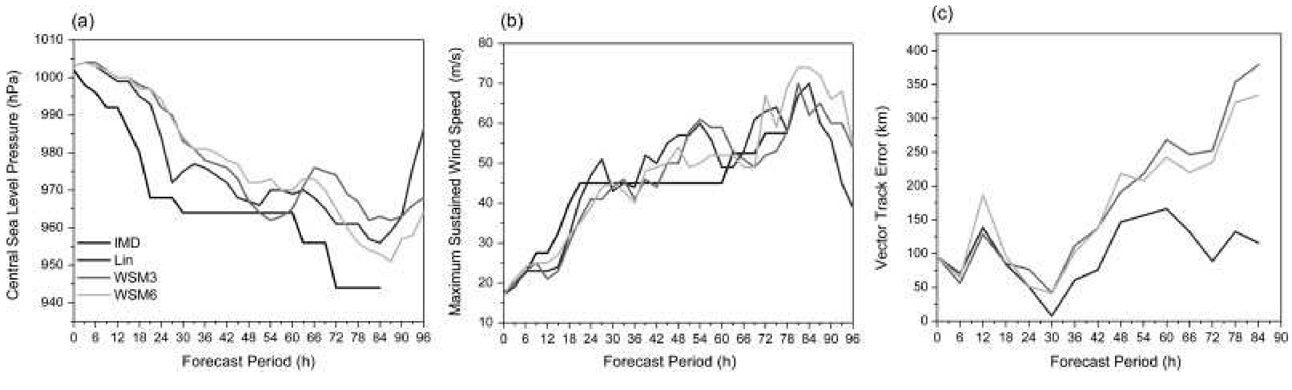

Figure 7. Time variation of simulated (a) central sea-level pressure (hPa), (b) maximum sustained winds (m s^{-1}) and (c) errors in track positions of cyclone Sidr for the experiments with different microphysics schemes, along with the IMD estimates.

produced the same intensity as WSM6 and better than WSM3.

4.3. *Sensitivity experiments with PBL schemes*

Here, the KF convection, LIN microphysics and NOAH surface schemes are held fixed as per previous results and the PBL simulations are varied according to the YSU, MYJ and ACM schemes. The mean error results for the five cyclones indicate that large intensity variation occurs with the different PBL schemes. The YSU scheme is found to produce minimum CSLP and wind errors than the other two schemes (Figure 3(b) and (c)). The time variation of CSLP and winds for cyclone Sidr from experiments

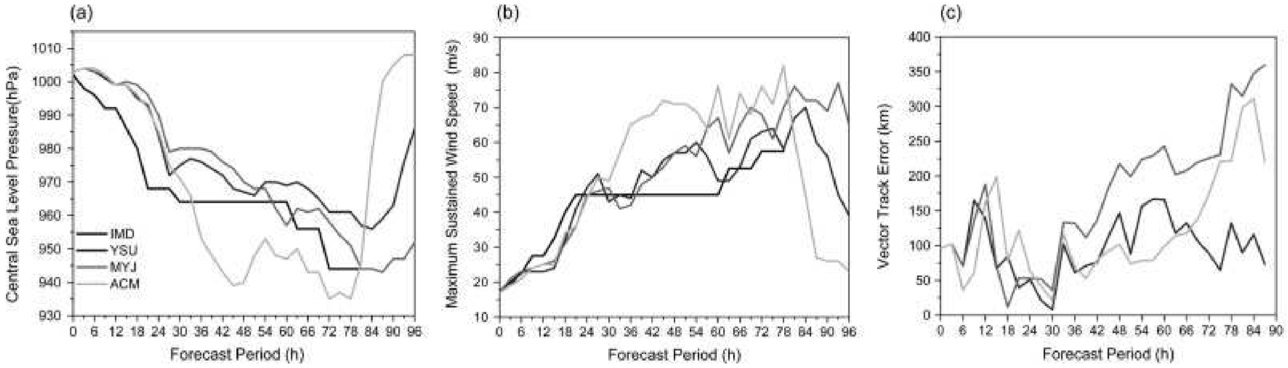

Figure 8. Time variation of simulated (a) central sea-level pressure (hPa), (b) maximum sustained winds (m s^{-1}) and (c) errors in track positions of cyclone Sidr for experiments with different PBL schemes, along with the IMD estimates.

using the different PBL schemes (Figure 8) indicates that the ACM scheme produces the highest intensification of the storm with a CSLP of 933 hPa and with maximum winds of 65 m s^{-1}. However, this is an overestimation of the actual intensity. The ACM experiment shows two peaks in intensification, one at 42 h and the second at 78 h, with an intermittent weakening phase between them. The YSU and MYJ experiments produced nearly similar trends in CSLP. Both the YSU and MYJ schemes have a deepening period of 84 h that is slightly higher than the observed deepening period (72 h). The IMD estimates indicate that the attained minimum CSLP is 945 hPa and the maximum winds are 58 m s^{-1} at the mature stage. The minimum CSLP at the mature stage of the storm was 955 hPa and 945 hPa with the YSU and MYJ schemes respectively. The time series of maximum winds with the YSU scheme are closer to reported values throughout the simulation. The MYJ scheme produced nearly similar trends of winds as the YSU scheme till 55 h, but overestimated the winds thereafter. The maximum winds simulated with ACM, MYJ and YSU at the mature stage of the storm are 80 m s^{-1}, 75 m s^{-1} and 68 m s^{-1} respectively. The time series of maximum winds indicates that the ACM scheme significantly overestimates the maximum winds throughout the simulation. Azimuthally averaged radius–height sections of tangential winds from the three simulations (Figure 9) shows stronger lower level winds (> 40 m s^{-1}) in the inflow region and a stronger wind maximum (60–100 m s^{-1}) extending vertically up to 13 km, up to 11 km and up to 8 km with the ACM, MYJ and YSU schemes respectively. The YSU scheme seems to produce relatively weaker tangential winds than the other two PBL schemes, in better agreement with reported values. The variation in the intensity of the storm with the three PBL schemes is related to the differences in the parametrization of turbulence exchange/drag coefficient in the respective schemes. The eddy diffusivity is derived from TKE and a length scale in the MYJ scheme and from friction velocity and PBL height in the YSU and ACM schemes. The higher intensification in the MYJ simulation is due to higher turbulence exchange coefficients simulated with schemes using TKE as compared with the simple first-order non-local schemes such as YSU, as reported in Hill *et al.* (2009). The present results corroborate the findings from the earlier work of Nolan *et al.* (2009a, 2009b) based on comparisons of high-resolution WRF simulations for hurricane Esabel (2003) using observations obtained from the Coupled Boundary Layer and Air–Sea Transfer Experiment (CBLAST). In their study it was found that the MYJ scheme consistently produces larger frictional tendencies in the boundary layer than the YSU scheme, leading to a stronger low-level inflow and a stronger wind maximum at the top of the boundary layer, thus simulating more intensive storms than with the YSU scheme.

The vector track errors are nearly similar with the three PBL schemes till 48 h but are drastically different thereafter. The track errors with the ACM and MYJ schemes are about 25–40% higher than those with the YSU scheme after 48 h (Figure 3(a)). Overall, the YSU scheme produced minimum track errors throughout the simulation time. This is also seen from the time series of the track errors for cyclone Sidr with various PBL schemes (Figure 8(c)). Thus the combination of the KF scheme for convection, the LIN scheme for microphysics and the YSU PBL scheme produced the best simulation of intensity and track.

4.4. *Sensitivity experiments with surface physics schemes*

In this set of experiments the KF, LIN and YSU schemes are used as per previous results and the land surface schemes are varied according to the NOAH, SOIL and RUC schemes. Mean errors (IMD values minus model values) for the simulation experiments of five cyclones with all thee surface schemes indicate underestimation of CSLP and overestimation of winds, suggesting higher intensification in simulations (Figure 3(a) and (b)). However, the errors are least with the NOAH scheme for both CSLP and winds. The time series of CSLP distribution for cyclone Sidr (Figure 10(a)) shows that the experiments with the NOAH and SOIL schemes produced almost a similar CSLP pattern, whereas the RUC experiment shows relatively higher CSLP throughout the simulation, attaining a minimum CSLP of 965 hPa at the mature stage of the storm.

The time series of the maximum sustained winds indicates that the SOIL scheme produces higher winds and the RUC scheme produces lower winds relative to observations during the deepening stage and mature stage of the storm. The maximum winds produced with the NOAH scheme agree more closely with the observations throughout the simulation than the other two schemes. The differences in simulated storm wind speeds among the three surface schemes is related to the variation in the surface flux parametrization and the related details in computation.

The mean track errors of the five cyclones with different surface schemes are almost similar till 48 h of integration (Figure 3(a)) and subsequently relatively higher with the

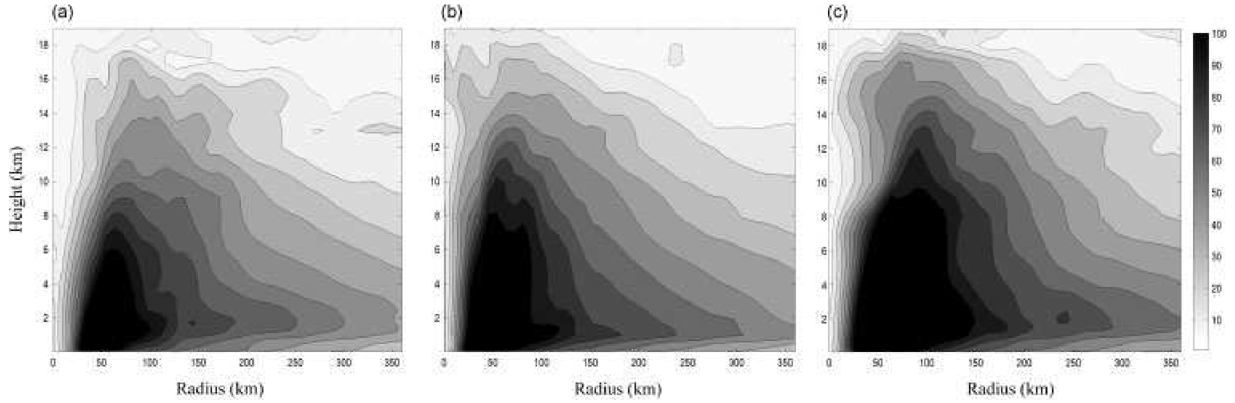

Figure 9. Depiction of the azimuthally averaged radius-height cross section of tangential wind (ms^{-1}) from experiments with different PBL schemes ((a) YSU, (b) MYJ and (c) ACM) at mature stage of cyclone Sidr corresponding to 0000 UTC on 15 November 2007. The scale on the *y* axis is height (km) and on the *x* axis is distance (km).

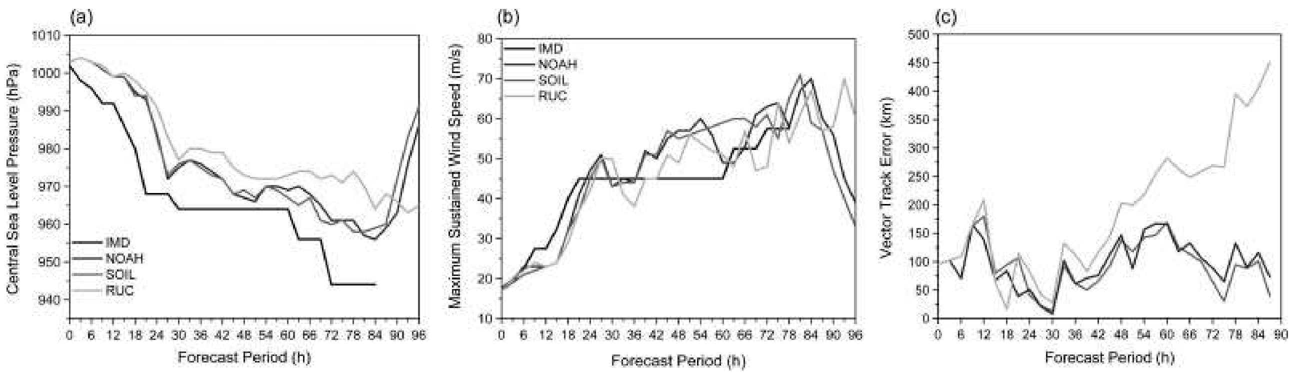

Figure 10. Time variation of simulated (a) central sea-level pressure (hPa), (b) maximum sustained winds (m s^{-1}) and (c) errors in track positions of cyclone Sidr for experiments with different land-surface model schemes along with IMD estimates.

RUC and SOIL schemes. The NOAH scheme produced minimum track errors for different integration periods, which are about 10–40% less than those with the RUC and SOIL experiments. From the time series of track errors for cyclone Sidr (Figure 10(c)) it is noted that all three surface schemes produce similar magnitude track errors till 40 h of simulation and thereafter the RUC scheme produces significantly larger errors than the other two schemes. The NOAH scheme is observed to be the best due to better estimation of intensity, although less track errors are noticed with both the NOAH and SOIL schemes. Thus the combination of KF for convection, LIN for microphysics, YSU for PBL and NOAH for surface processes are observed to produce the best simulation for intensity and track predictions.

An important result from the sensitivity experiments is that the minimum errors for track and intensity are associated with the ensemble mean (represented by the solid lines in Figure 3) from the five storms based on the 65 ensemble members of different physics variants. The ensemble mean of all the physics experiments is noted to provide a better estimate for both track and intensity when compared to individual forecasts. The ensemble mean errors are found to be of the order of 2.2, −1.2, −2.9 and 11 m s^{-1} for intensity and 125, 253, 317 and 419 km for vector track position at 24, 48, 72 and 96 h forecasts respectively. This indicates the importance of physics ensembles for intensity predictions, especially when using a coarse resolution model (9 km inner domain) with a parametrized convection scheme.

5. Track and intensity errors

Results of simulations made with the best model physics (KF for CC, LIN for CMP, YSU for PBL and NOAH for LSM) for 21 cyclones are presented here. The time series of errors (IMD value minus model value), mean error (ME) and standard deviation (SD) in respect of CSLP, maximum winds and the track positions are presented in Figure 11. The mean errors for CSLP (Figure 11(a)) indicate underestimation, varying as marginal (±1 hPa) in the initial stages up to 18 h, increase gradually during the deepening stage to 15 hPa at 54 h and then reduce to 12 hPa at 72 h when the storm approaches the land region. The RMSE and SD in CSLP increase from 7 hPa/5 hPa at 12 h to 21 hPa/17 hPa at 72 h of the simulation period. Correspondingly the ME and RMSE in maximum winds are marginal (−4 m s^{-1}/8 m s^{-1}) during the initial stages and increase gradually during the deepening and landfall stages (−17 m s^{-1}/25.7 m s^{-1}) at 72 h, indicating higher intensification of simulated storms (Figure 11(b)). The value of SD for maximum winds varies between 11 and 19 m s^{-1} during the 72 h forecast period.

The mean vector track error (Figure 11(c)) and its RMSE progressively increase from 122 km/160 km at 12 h to 244 km/297 km during the deepening phase (48 h) and to 249 km/337 km during the land fall (72 h) stage. These track errors are smaller than the corresponding mean errors obtained with the quasi-Lagrangian model model for the BOB region, which were reported to vary from 103 km to 415 km at 12 h to 72 h of prediction (Prasad, 2006; Prasad and Rama Rao, 2006) from simulations of 13 cyclones that

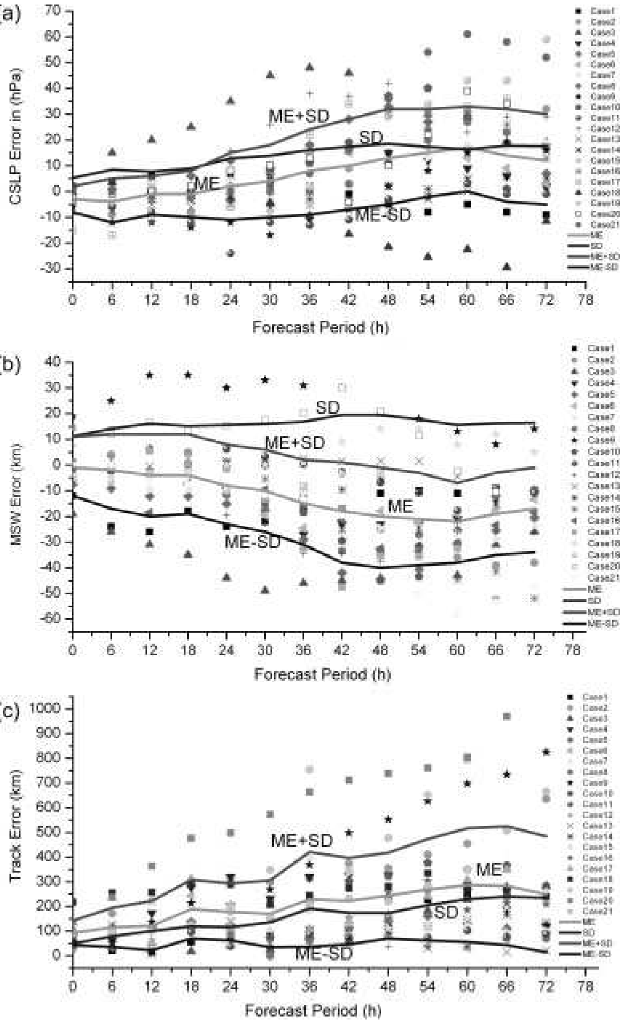

Figure 11. Mean error (ME), standard deviation (SD), ME + SD and ME − SD in (a) central sea-level pressure (hPa), (b) maximum sustained winds (m s^{-1}) and (c) errors in track positions for the 21 cyclones.

formed over BOB between 1997 and 2006. The standard deviation in track positions varies from 115 km at 24 h to 235 km during the deepening, mature and decay phases (72 h). In the present experiments, the mean error in the initial position of the cyclone vortex is about 85 km, which is because of the conditions defined from the coarse NCEP GFS 1° latitude/longitude analysis and no vortex initialization is included. Given these initial position errors, the errors in the simulation (varying from 122 km to 250 km between 12 and 72 h of simulation) could be assumed to be less by 20–40% and so are considerably smaller than operational forecast errors. Of the 21 cyclones studied the minimum error in track is 22 km as found for cyclone Fanoos (December 2005) and the maximum error is 820 km as found for the recurving storm Nargis (April 2008).

Two error thresholds of ME + SD and ME − SD are applied for CSLP, maximum winds and track position error time series to identify the best simulated cases (Figure 11). Using this criterion, 14 cyclones (Thane, Jal, Ward, Aila, Nisha, Khaimuk, Rashmi, Akash, Sidr, Mala, Fanoos Baaz, Myanmar-04 and Machilipatnam) are found to be well simulated. For these 14 cyclones the ME, SD and RMSE in CSLP are observed to be of the order of 1, 5 and 10 hPa at 24 h to 10, 12 and 16 hPa at 72 h of forecast period respectively. The peak errors in CSLP (ME ∼16 hPa, RMSE∼23 hPa) occurred at about 48 h of model integration and coincide with deepening or sudden intensification of the storm in most cases. The ME, SD and RMSE in MSW for these selected cyclones are found to vary in the range of −8–12 m s^{-1} at 24 h to 18–20 m s^{-1} at 72 h. The ME, SD and RMSE in track positions are found to vary from 126, 75 and 170 km at 24 h to 134, 82 and 226 km at 72 h of prediction respectively. The minimum error in track is found to be 22 km for Fanoos cyclone and maximum error is found to be 280 km for Jal cyclone.

Of the 14 best cases of simulation four cyclones (Aila, Rashmi, Akash, Sidr) that moved northward, five (Thane, Jal, Nisha, Khaimuk, Machilipatnam Dec,03) northwestward, three (Ward, Fanoos, Baaz) westward and two (Mala, Mynmar-04) in northeastward directions (Table 1). It is noted that of these, ARW modelling has shown better prediction skills for northward and northwestward moving cyclones as compared with the westward and northeastward moving cyclones. The mean error for the northward moving cyclones is found to vary from −2 to 10.2 hPa in CSLP, −6 to −14 m s^{-1} in maximum winds and 80 to 85 km in track position corresponding to 24–72 h forecasts. For the northeastward moving cyclones the errors are found to vary from 11 to 28 hPa in CSLP, −14 to −24 m s^{-1} and 211 to 324 km in track positions corresponding to 24–72 h forecasts. The mean errors for westward moving storms are noted to vary from −5 to 4 hPa in CSLP, 1 to −13 m s^{-1} in maximum winds and 154 to 274 km in track positions. For the northwestward moving storms the errors are about 1–11 hPa in CSLP, −8 to −14 m s^{-1} in maximum winds and 101–187 km in track positions corresponding to 24–72 h forecasts. The mean errors suggest that the northward moving cyclones are simulated the best, followed by the northwestward, westward and northeastward moving cyclones, with respect to vector track as well as intensity estimates.

Simulated low vector-track errors in respect of northward/northwestward moving storms may be explained through the effect of increasing Coriolis force with latitude (i.e. the β parameter), which gives a relatively higher contribution to the steering force controlling the movement of the cyclone when the system drifts to higher latitudes. A similar explanation holds for the west and northeast moving cyclone systems, as these were found to form at lower latitudes and the model dynamics has deficiencies to balance the forces with low Coriolis force magnitude.

For the seven cyclones not well simulated (Laila, Nargis, Pyarr, Mynmar-04, Bangladesh-02, Cuddalore and Bangladesh-00) the mean errors varied from −2 to 29 hPa in CSLP, 3 to −23 m s^{-1} in maximum winds and 280 to 530 km in track positions. Most of these storms are northeastward moving ones, except Laila, Pyarr, and Cuddlore 2000, which supports the prior explanation. In this the maximum errors in track at landfall time are noted to be 824 km (Nargis), 634 km (Laila) and 960 km (Cuddalore 2000).

Cyclones Sidr, Nargis, Khaimuk and Nisha representing storms moving in the northward, northeastward, northwestward directions were analysed by model simulation to produce track, intensity and wind distributions associated with the predicted storm. The errors in CSLP for the cyclone Sidr range from −2 to −14 hPa and errors in maximum winds vary from −2 to 10 m s^{-1} for the 24–72 h forecast period (Figure 12). It is seen that vector track distances for cyclone Sidr are simulated very accurately by the ARW

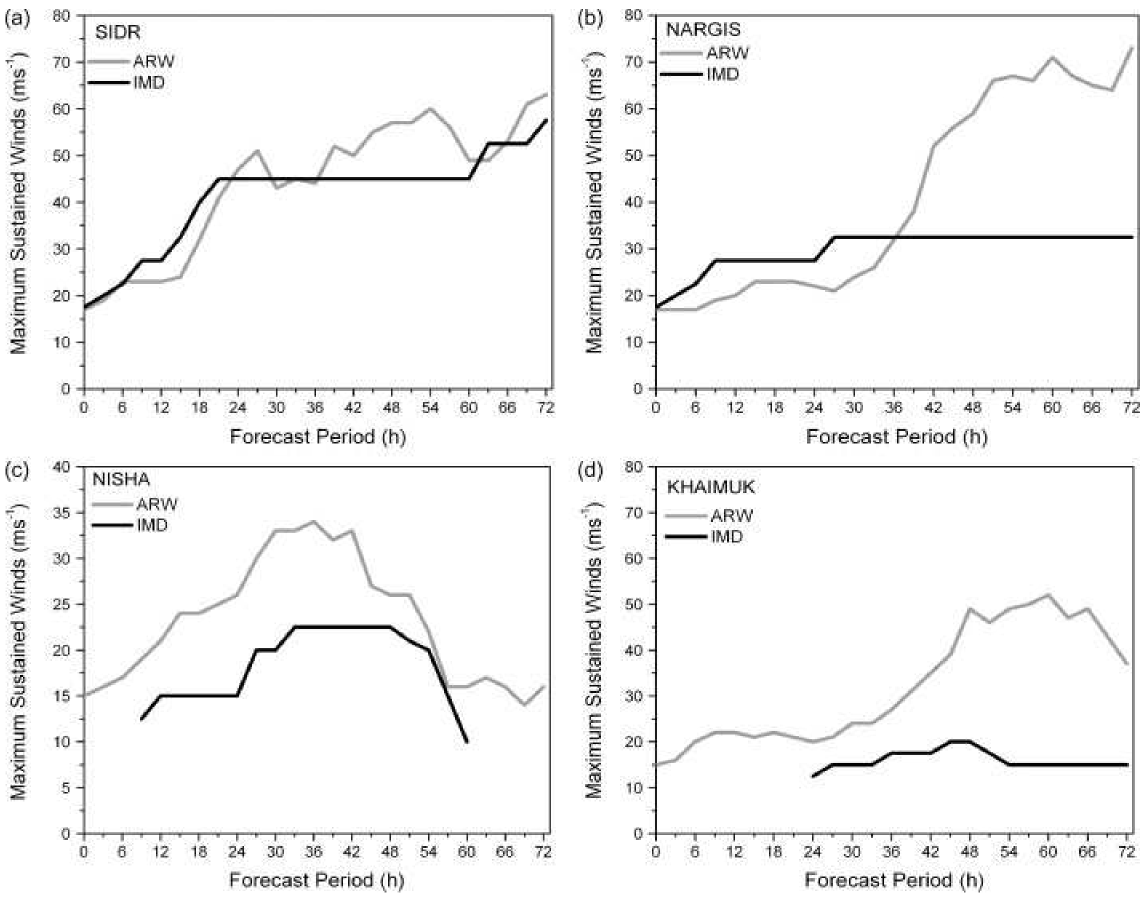

Figure 12. Simulated maximum sustained winds along with the IMD estimates for the cyclones (a) Sidr, (b) Nargis, (c) Nisha and (d) Khaimuk.

model, varying from 100 km at 24 h to 130 km at 72 h of the forecast period (Figure 13). The simulated landfall point for cyclone Sidr is very near and in a range of about 70 km from the observed landfall point (21.5°N, 89.8°E).

The CSLP errors for cyclone Nargis are observed to range from −12 hPa at 24 h to 19 hPa at 72 h and the errors in maximum winds vary from 30 m s^{-1} at 24 h to 14 m s^{-1} at 72 h. The vector track errors for cyclone Nargis are found to increase progressively from 200 km at 24 h to 820 km at 72 h, which is evident from the deviation of the simulated track by 800 km north of the actual landfall point (16°N, 94.5°E) in Myanmar.

The vector track errors for cyclone Nisha are found to range from 100 km at 24 h to 90 km at 72 h and indicate marginal error, with the simulated landfall point deviating by about 85 km south of the actual landfall point (11.30°N, 79.80°E near Karaikal Tamilnadu). The CSLP and wind errors for cyclone Nisha are found to vary from −2 hPa/−9.5 m s^{-1} at 24 h, to 9 hPa/−20 m s^{-1} at 72 h forecast period.

For cyclone Khaimuk the simulated track errors varied between 78 km at 24 h and 75 km at 72 h of simulation, which indicate very marginal errors, with the predicted landfall point deviating by 100 km northeast of the observed landfall point (15.2°N, 80.2°E near Kavali, Andhra Pradesh). The CSLP and wind errors of cyclone Khaimuk are found to vary from 2 hPa/−7.5 m s^{-1} at 24 h to $-22ms^{-1}$/17 hPa at 72 h.

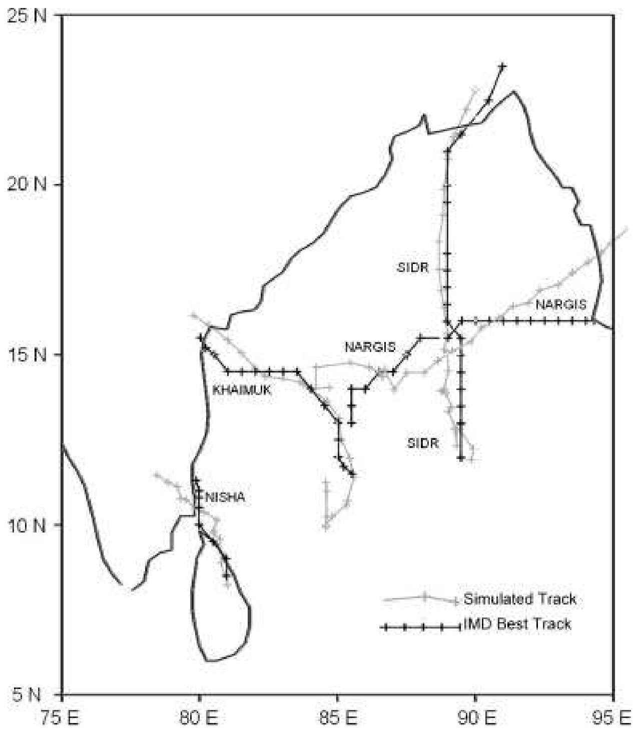

Figure 13. Simulated and observed tracks of the cyclones Sidr, Nargis, Nisha and Khaimuk.

While the intensity (CSLP, MSW) could be very nearly simulated in the case of cyclone Sidr, it is overestimated for cyclones Nargis, Nisha and Khaimuk (Figure 12). The simulated track positions indicate that the modelling could very accurately estimate the landfall point of cyclones Sidr, Nisha and Khaimuk, but it produced a relatively large error

Table 2. Comparison of the structure parameters for six tropical cyclones.

Cyclone	Maximum reflectivity (dBz)		Maximum surface winds (m s^{-1})			Radius of maximum winds (km)		Core warming (ΔT) K	
	ARW	DWR	ARW	IMD	CIRA	ARW	CIRA	ARW	CIRA
Sidr (1100 UTC, 15 November 2007)	48	37	60	50	62	34	20.5	4	3
Nisha (1200 UTC, 26 November 2008)	35	37	32	22	25.5	40	43	5	2
Khaimuk (0000 UTC, 15 November 2008)	45	39	35	20	24	30	33	3	2
Nargis (1400 UTC, 2 May 2008)	–	–	45	35	53	44	30	3	4
Jal (0000 UTC, 7 November 2010)	46	44	45	28	37	50	61	4	2
Thane (1200 UTC, 29 December 2011)	39	42	43	37.5	38	33	33	4	3

ARW, ARW model results; CIRA, data from CIRA analyses; DWR, reflectivity data from IMD DWR; IMD, IMD MSW estimates.

in the landfall point for cyclone Nargis, which had more recurvature at lower latitude than is normal. It is to be noted that the small number of samples considered in the present analysis based on track direction is not adequate to derive statistical significance, and so the results are used to only provide qualitative indications. Hence the error estimates for the above subsets of cyclones based on track direction have to be viewed within this limitation.

6. Structure

Simulated total cloud fractions, maximum reflectivity and accumulated 24 h rainfall at landfall time are compared with available observations from satellite imagery, doppler weather radar (DWR) reflectivity and TRMM rainfall for cyclones Sidr, Nargis, Khaimuk and Nisha in order to examine cloud band organization and rainfall. The ARW model is able to reproduce the cloud pattern associated with each of the above cyclones reasonably well. Formation of comma cloud bands with circular symmetry at 15 UTC on 15 November 2007 for Sidr, 0900 UTC on 15 November 2008 for Khaimuk and 19 UTC 26 November 2008 for Nisha in the simulation was in good comparison with Kalpakana-1 infrared images. The alignment of convective cloud bands in the north sector for cyclones Sidr and Khaimuk, and in the north, east and southeast sectors for cyclones Nargis and Nisha was simulated as in satellite imagery (not shown). The model-derived 24 h accumulated rainfall location and distribution at landfall for the four cyclones was in good agreement with corresponding TRMM data. The rainfall distribution of 80–200 mm with northward organization of rain bands for Sidr, northeastward rain bands of 60–180 mm for Nargis, northward and northeastward rain bands of 20–160 mm for Khaimuk and Nisha are found to be well simulated according to the TRMM data.

A quantitative comparison of the structure of six simulated cyclones is made with data from Multi-Platform Tropical Cyclone Surface Wind Analysis (Knaff *et al.*, 2011) products created by NOAA/NESDIS/STAR (http://rammb.cira.colostate.edu/products/tc_realtime). The maximum surface wind, radius of maximum winds (RMW), maximum warming in the core region (i.e. temperature anomaly) and maximum reflectivity of the clouds in the cyclone region were found to compare with the observational estimates with a mean error of 7.4% for reflectivity, 14% for maximum winds, 13% for RMW and 30% for warming (Table 2) for the six cyclones considered, wherein the MW is generally overestimated as compared to the IMD wind data; RMW is overestimated/underestimated for one cyclone each; warm core is overestimated for one cyclone; and reflectivity is overestimated for two cyclones. In summarily, the wind, cloud and thermal structures of the cyclones under study were well simulated by ARW model.

7. Summary and Conclusions

In this study the performance of the ARW mesoscale model with 9 km resolution is evaluated in a statistical sense for the operational prediction of TCs in the BOB region by considering 21 cyclones during 2000–2011 and evaluating their intensity and track parameters. The results of 65 sensitivity experiments varying the convection, microphysics, boundary layer turbulence and land surface parameterization for five severe cyclones (Sidr, Khaimuk, Nargis, Jal, Thane) indicated the forecasts of intensity and track are highly sensitive to the model physics and that the combination of KF convection, LIN microphysics, YSU PBL and NOAH surface physics options provide the best physics for operational forecasting with least errors. Whereas the convection and PBL parametrizations produced a large impact, microphysics and land surface physics schemes made minimum impact on the intensity and track predictions. The KF scheme produced more realistic intensity and track positions with relatively higher convective warming and stronger vertical motions in the upper troposphere relative to the other cumulus schemes, which may be due to triggering of convection based on buoyancy in the case of the KF scheme. Large changes in intensity are noted with variation of PBL schemes. Whereas ACM and MYJ overestimated the intensity during deepening and mature cyclone stages, the YSU scheme offered realistic intensity estimates because of realistic simulation of winds in the cyclone inflow region through suitable diffusivity.

The ensemble mean of all the physics sensitivity experiments is found to provide a better estimate for track as well as intensity when compared with individual forecasts, emphasizing the importance of physics ensembles for intensity predictions when using a coarse resolution (9 km) and parametrized convection scheme. Results of simulations of 21 cyclones using the best physics parametrizations indicated that the model generally overestimates the intensity of cyclones with a mean error ranging from −2 to 15 hPa for CSLP and −1 to −22 m s^{-1} for MSW from 24 to 72 h predictions. The mean vector position error is found to vary from 122 km at 24 h to 250 km at 72 h. Although cyclone Fanoos had the least error of 22 km, Nargis had the maximum error of 800 km in vector track position at landfall. With an initial error of 80 km in the position, the error estimates for CSLP, MSW and vector position clearly demonstrate that the model performance is reasonably good for the prediction of tropical cyclones in the BOB and comparably better than the operational forecasts by the IMD quasi-Lagrangian model. About 67% of the cyclones are simulated with mean errors in CSLP, MSW and vector track distances within ± 1 SD. The movement of northward/northwestward tracking storms is better simulated as compared with the westward and northeastward moving cyclones, perhaps due to the increasing influence of the Coriolis force on the motion of the cyclone at higher latitudes.

The operational HWRF in NCEP uses 3 km resolution (27 km: 9 km: 3 km) without cumulus parametrization scheme in the 3 km domain, and the recent study by Gopalakrishnan *et al.* (2012) indicated that a 3 km domain produces more accurate intensity and structure of the cyclones in forecasts. A caveat in the present study with 9 km resolution is that the results are dependent on the parametrized convection. Although it is desirable to resolve the convection with sufficiently high resolution and with the use of explicit cloud physics, this would involve enormous computational and runtime overheads, which may be a constraint on real-time operational predictions in the Indian context. A critical requirement for operational purpose is to obtain real-time forecasts with faster turn around and with reasonable accuracy. Although the present study has a limitation in the number of cyclone case studies, due to the occurrence of fewer storms over the BOB region as compared with the Atlantic and Pacific oceans, the results from the present study would be useful for planning real-time predictions using AWR modelling system. Another interesting aspect is that although the model boundary conditions in the present study for some of the old storms (for years 2000 to 2004) were obtained from the GFS analysis, the results clearly indicate that a large difference in the error statistics was not produced, which was evident from a comparison of the mean forecast errors from the five cases (cyclones Khaimuk, Nargis, Sidr, Jal and Thane) for ensembles where the forecast boundary conditions were used. This study demonstrates the advantages of the modelling systems and their use in the application of ensemble prediction methodology for real-time prediction of TCs over the NIO basin at the resolution of 9 km.

Acknowledgement

The authors thank Sri S. C. Chetal, Director, IGCAR, for his encouragement and support. Public access of the WRF-ARW model, real-time GFS analysis and forecasts and TRMM rainfall data by NCAR, NCEP and NASA (USA) are gratefully acknowledged. The India Meteorological Department is acknowledged for providing the best track and intensity estimates and the DWR reflectivity composites of tropical cyclones. The authors acknowledge the anonymous reviewers for providing critical reviews and valuable comments, which helped to improve the manuscript.

References

Arakawa A, Schubert WH. 1974. Interaction of a cumulus cloud ensemble with the large-scale environment. Part I. *J. Atmos. Sci.* **31**: 674–701.

Bender MA, Ginis I, Tuleya RE, Thomas B, Marchok T. 2007. The operational GFDL coupled hurricane–ocean prediction system and a summary of its performance. *Mon. Weath. Rev.* **135**: 3965–3989.

Betts AK, Miller MJ. 1986. A new convective adjustment scheme. Part II: Single column tests using GATE wave, BOMEX, and Arctic air-mass data sets. *Q. J. R. Meteorol. Soc.* **112**: 693–709.

Bhaskar Rao DV, Naidu CV, Srinivasa Rao B. 2001. Trends and fluctuations of the cyclonic systems over North Indian Ocean. *Mausam* **52**(1): 1–8.

Bhaskar Rao DV, Hari Prasad D. 2006. Numerical prediction of the Orissa super-cyclone: Sensitivity to the parameterization of convection, boundary layer and explicit moisture processes. *Mausam* **57**(1): 61–78.

Bhaskar Rao DV, Hari Prasad D. 2007. Sensitivity of tropical cyclone intensification to boundary layer and convective processes. *Nat. Hazards* **41**(3): 429–445.

Bhaskar Rao DV, Hari Prasad D, Srinivas D. 2009. Impact of horizontal resolution and the advantages of the nested domains approach in the prediction of tropical cyclone intensification and movement. *J. Geophys. Res.* **114**: D11106, 24–pp. DOI:10.1029/2008JD011623.

Chen F, Dudhia J. 2001. Coupling an advanced land-surface/hydrology model with the Penn State/NCAR MM5 modeling system. Part I: Model description and implementation. *Mon. Weath. Rev.* **129**: 569–585.

Davis C, Wang W, Chen SS, Chen Y, Corbosiero K, De Maria M, Dudhia J, Holland G, Klemp J, Michalakes J, Reeves H, Rotunno R, Snyder C, Xiao O. 2008. Prediction of landfalling hurricanes with the Advanced Hurricane WRF model. *Mon. Weath. Rev.* **136**: 1990–2005.

Deshpande M, Pattnaik S, Salvekar PS. 2010. Impact of physical parameterization schemes of numerical simulation of super cyclone Gonu. *Nat. Hazards* **55**: 211–231. DOI 10.1007/s11069-010-9521-x.

Dudhia J. 1989. Numerical study of convection observed during winter monsoon experiment using a mesoscale two-dimensional model. *J. Atmos. Sci.* **46**: 3077–3107.

Dudhia J. 1996. *A Multi-layer Soil Temperature Model for MM5*. Preprint from the Sixth PSU/NCAR Mesoscale Model Users' Workshop.

Dudhia J, Hong S-Y, Lim KS. 2008. A new method for representing mixed-phase particle fall speeds in bulk microphysics parameterizations. *J. Meteorol. Soc. Jpn* **86A**: 33–44.

Gopalakrishnan SG, Goldenberg S, Quirino T, Zhang X, Marks F, Yeh KS, Atlas R, Tallapragada V. 2012. Toward improving high-resolution numerical hurricane forecasting: Influence of model horizontal grid resolution, initialization, and physics. *Wea. Forecast.* **27**: 647–666.

Gray WM. 1968. Global view of the origin of tropical disturbances and storms. *Mon. Weath. Rev.* **96**: 669–700.

Grell GA, Dévényi D. 2002. A generalized approach to parameterizing convection combining ensemble and data assimilation techniques. *Geophys. Res. Lett.* **29**(14): 1693. DOI:10.1029/2002GL015311.

Hill KA, Lackmann GM. 2009. Analysis of idealized tropical cyclone simulations using the weather research and forecasting model: sensitivity to turbulence parameterization and grid spacing. *Mon. Weath. Rev.* **137**: 745–765.

Holtslag AAM, Boville BA. 1993. Local versus non-local boundary layer diffusion in a global climate model. *J. Climate* **6**: 1825–1842.

Hong S-Y, Dudhia J, Chen S-H. 2004. A revised approach to ice microphysical processes for the bulk parameterization of clouds and precipitation. *Mon. Weath. Rev.* **132**: 103–120.

Hong S-Y, Noh Y, Dudhia J. 2006. A new vertical diffusion package with explicit treatment of entrainment processes. *Mon. Weath. Rev.* **134**: 2318–2341.

India Meteorological Department. 2010. *Reports on Cyclonic Disturbances over North Indian Ocean*. Regional Specialised Meteorological Centre-Tropical Cyclones: New Delhi. http://www.imd.gov.in/section/nhac/dynamic/rsmc1.htm

Janjić ZI. 1994. The step-mountain eta coordinate model: Further developments of the convection, viscous sublayer and turbulence closure schemes. *Mon. Weath. Rev.* **122**: 927–945. DOI:10.1175/1520-0493.

Janjić ZI. 2000. Comments on 'Development and evaluation of a convection scheme for use in climate models'. *J. Atmos. Sci.* **57**: 3686.

Janjić ZI. 2002. *Nonsingular Implementation of the Mellor–Yamada Level 2.5 Scheme in the NCEP Meso Model*. Office Note, No. 437, NCEP: 61 pp.

Kain JS. 2004. The Kain–Fritsch convective parameterization: An update. *J. Appl. Meteorol.* **43**: 170–181.

Knaff JA, DeMaria M, Molenar DA, Sampson CR, Seybold MG. 2011. An automated objective, multiple-satellite-platform tropical cyclone surface wind analysis. *J. Appl. Meteorol. Climatol.* **50**: 2149–2166.

Krishna KO, Routray A, Mohanty UC, Kulkarni MA. 2010. Simulation of tropical cyclones over Indian Seas: Data impact study using WRF-Var assimilation system. In *Indian Ocean Tropical Cyclones and Climate Change*, Charabi Y (ed.). Springer-Verlag: Berlin; 115–124.

Krishna KO, Mohanty UC, Routray A, Kulkarni MA, Mohapatra M. 2012. Customization of WRF-ARW model with physical parameterization schemes for the simulation of tropical cyclones over North Indian Ocean. *Nat. Hazards* **63**(3): 1337–1359.

Lin YL, Farley RD, Orville HD. 1983. Bulk parameterization of the snow field in a cloud model. *J. Appl. Meteorol.* **22**: 1065–1092.

Marks FD, Shay LK. 1998. Landfalling tropical cyclones: Forecast problems and associated research opportunities. *Bull. Am. Meteorol. Soc.* **79**: 305–323.

McNoldy B, DeMaria M, Tallapragada V, Marchock T. 2010. WRF performance diagnostics form the 2009 atlantic hurricane season. Preprints, *American Meteorological Society 29th Conference on Hurricanes and Tropical Meteorology*, Tucson, AZ.

Mellor GL, Yamada T. 1982. Development of a turbulence closure model for geophysical fluid problems. *Rev. Geophys. Space Phys.* **20**: 851–875.

Mohanty UC, Mandal M, Raman S. 2004. Simulation of Orissa super-cyclone (1999) using PSU/NCAR mesoscale model. *Nat. Hazards* **31**: 373–390.

Mlawer EJ, Taubman SJ, Brown PD, Iacono MJ, Clough SA. 1997. Radiative transfer for inhomogeneous atmosphere: RRTM, a validated correlated-k model for the longwave. *J. Geophys. Res.* **102**(D14): 16663–16682.

Mukhopadhyay P, Taraphdar S, Goswami BN. 2011. Influence of moist processes on track and intensity forecast of cyclones over the north Indian Ocean. *J. Geophys. Res.* **116**: D05116, 21–pp. DOI:10.1029/2010JD014700.

Nolan DS, Zhang JA, Stern DP. 2009a. Evaluation of planetary boundary layer parameterizations in tropical cyclones by comparison of *in situ* observations and high-resolution simulations of hurricane Isabel (2003). Part I: Initialization, maximum winds, and the outer-core boundary layer. *Mon. Weath. Rev.* **137**: 3651–3674.

Nolan DS, Stern DP, Zhang JA. 2009b. Evaluation of planetary boundary layer parameterizations in tropical cyclones by comparison of in situ observations and high-resolution simulations of hurricane Isabel (2003). Part II: Inner-core boundary layer and eyewall structure. *Mon. Weath. Rev.* **137**: 3675–3698.

Pattanaik S, Mohanty UC. 2008. A comparative study on performance of MM5 and WRF models in simulation of tropical cyclones over Indian seas. *Current Sci.* **95**(7): 923–936.

Pattanaik S, Mohanty UC. 2010. Simulation of track and intensity of Gonu and Sidr with WRF-NMM modeling system. In *Indian Ocean Tropical Cyclones and Climate Change*, Charabi Y (ed.). Springer-Verlag: Berlin; 83–92.

Pleim JE. 2007. A combined local and non-local closure model for the atmospheric boundary layer. Part 1: Model description and testing. *J. Appl. Meteorol. Climatol.* **46**: 1383–1395.

Prasad K. 2006. Further experiments on cyclone track prediction with quasi-Lagrangian limited area model. *Meteorology and Atmospheric Physics.* **91**(1–4): 183–199.

Prasad K, Rama Rao YV. 2003. Cyclone track prediction by a quasi-Lagrangian model. *Meteorol. Atmos. Phys.* **83**: 173–185.

Prasad K, Rama Rao YV. 2006. *Simulation Studies on Cyclone Track Prediction by Quasi-Lagrangian Model (QLM) in Some Historical and Recent Cases in the Bay of Bengal, Using Global Re-analysis and Forecast Grid Point Data Sets*. SMRC-No15, SAARC Meteorological Research Centre: Dhaka, Bangladesh.

Raghavan S, Sen Sarma AK. 2000. Tropical cyclone impacts in India and neighbourhood. In *Storms*, Vol. 1, Pielke R Jr, Pielke R Sr (eds). Routledge: London; 339–356.

Raju PVS, Jayaraman P, Mohanty UC. 2011a. Sensitivity of physical parameterizations on prediction of tropical cyclone Nargis over the Bay of Bengal using WRF model. *Meteorol. Atmos. Phys.* **113**(3–4): 125–137. DOI: 10.1007/s00703-011-0151-y.

Raju PVS, Jayaraman P, Mohanty UC. 2011b. Prediction of severe tropical cyclones over the Bay of Bengal during 2007–2010 using high-resolution mesoscale model. *Nat. Hazards.* DOI: 10.1007/s11069-011-9918-1.

Rama Rao YV, Prasad K. 2005. *Further Evaluation of Quasi-Lagrangian Model*. SMRC-No. 12, SAARC Meteorological Research Centre: Dhaka, Bangladesh.

Rapport EN, Franklin JL, Avila LA, Baig SR, Beven II JL, Blake ES, Burr CA, Jiing JG, Juckins CA, Knabb RD, Landsea CW, Mainelli M, Mayfield M, McAdie CJ, Pasch RJ, Sisko C, Stewart SR, Tribble AN. 2009. Advances and challenges at the National Hurricane Center. *Wea. Forecast.* **24**: 395–419.

Singh R, Pal PK, Kishtawal CM, Joshi PC. 2008. The impact of variational assimilation of SSM/I and QuikSCAT satellite observations on the numerical simulation of Indian Ocean tropical cyclones (2008). *Weath. Forecast.* **23**: 460–476.

Singh R, Kishtawal CM, Pal PK, Joshi PC. 2011. Assimilation of the multisatellite data into the WRF model for track and intensity simulation of the Indian Ocean tropical cyclones. *Meteorol. Atmos. Phys.* **111**(3–4): 103–119, DOI: 10.1007/s00703-011-0127-y

Singh R, Kishtawal CM, Pal PK, Joshi PC. 2012. Improved tropical cyclone forecasts over north Indian Ocean with direct assimilation of AMSU-A radiances. *Meteorol. Atmos. Phys.* **115**(1–2): 15–34. DOI: 10.1007/s00703-011-0165–5.

Skamarock WC, Klemp JB, Dudhia J, Gill DO, Barker DM, Dudha MG, Huang X, Wang W, Powers Y. 2008. *A Description of the Advanced Research WRF Version 30*. NCAR Technical Note NCAR/TN-475+STR, Mesocale and Microscale Meteorology Division, National Centre for Atmospheric Research: Boulder, CO; 113 pp.

Smirnova TG, Brown JM, Benjamin SG, Kim D. 2000. Parameterization of cold season processes in the MAPS land-surface scheme. *J. Geophys. Res.* **105**(D3): 4077–4086.

Srinivas CV, Venkatesan R, Bhaskar Rao DV, Hariprasad D. 2007. Numerical simulation of Andhra severe cyclone (2003): Model sensitivity to boundary layer and convection parameterization. *Pure Appl. Geophys.* **164**: 1–23.

Srinivas CV, Venkatesan R, Vesubabu V, Nagaraju C. 2010. Impact of assimilation of conventional and satellite meteorological observations on the numerical simulation of a Bay of Bengal tropical cyclone of Nov 2008 near Tamilnadu using WRF model. *Meteorol. Atmos. Phys.* **110**(1–2): 19–44.

Trivedi DK, Mukhopadhyay P, Vaidya SS. 2006. Impact of physical parameterization schemes on the numerical simulation of Orissa super cyclone (1999). *Mausam* **57**(1): 97–110.

Tyagi A, Bandyopadhyay BK, Mohapatra M. 2010. Monitoring and prediction of cyclonic disturbances over North Indian Ocean by Regional Specialised Meteorological Centre, New Delhi (India): Problems and prospective. In *Indian Ocean Tropical Cyclones and Climate Change*, Charabi Y (ed.). Springer-Verlag: Berlin; pp. 93–103.

Yeh KS, Zhang X, Gopalakrishnan S, Aberson S, Rogers R, Marks FD, Atlas R. 2011. Performance of the experimental HWRF in the 2008 hurricane season. *Nat. Hazards.* DOI 10.1007/s11069-011-9787-7.

Zhang X, Quirino TS, Gopalakrishnan S, Yeh KS, Marks FD, Goldenberg SB. 2011. HWRFX: Improving hurricane forecasts with high resolution modeling. *Comput. Sci. Eng.* **13**: 13–21.

